Published in final edited form as:
Acta Biomater. 2012 July ; 8(6): 2297–2306. doi:10.1016/j.actbio.2012.02.021.

Umbilical cord stem cells released from alginate-fibrin microbeads inside macroporous and biofunctionalized calcium phosphate cement for bone regeneration

Wenchuan Chen[a,b], **Hongzhi Zhou**[a,c], **Michael D. Weir**[a], **Chongyun Bao**[b], and **Hockin H.K. Xu**[a,d,e,f]

[a]Biomaterials & Tissue Engineering Division, Department of Endodontics, Prosthodontics and Operative Dentistry, University of Maryland Dental School, Baltimore, MD 21201, USA

[b]State Key Laboratory of Oral Diseases, West China College of Stomatology, Sichuan University, Chengdu, Sichuan 610041, China

[c]Department of Oral & Maxillofacial Surgery, School of Stomatology, Fourth Military Medical University, Xi'an, China

[d]Center for Stem Cell Biology and Regenerative Medicine, University of Maryland School of Medicine, Baltimore, MD 21201, USA

[e]Marlene and Stewart Greenebaum Cancer Center, University of Maryland School of Medicine, Baltimore, MD 21201, USA

[f]Dept. of Mechanical Engineering, Univ. of Maryland, Baltimore County, MD 21250, USA

Abstract

The need for bone repair has increased as the population ages. The objectives of this study were to (1) develop a novel biofunctionalized and macroporous calcium phosphate cement (CPC) containing alginate-fibrin microbeads encapsulating human umbilical cord mesenchymal stem cells (hUCMSCs); and (2) investigate hUCMSC proliferation and osteogenic differentiation inside CPC for the first time. Macroporous CPC was developed using calcium phosphate powders, chitosan, and gas-foaming porogen. Five types of CPCs were fabricated: CPC control, CPC + 0.05% fibronectin (Fn), CPC + 0.1% Fn, CPC + 0.1% Arg-Gly-Asp (RGD), and CPC + 0.1% Fn + 0.1% RGD. Alginate-fibrin microbeads containing 10^6 hUCMSCs/mL were encapsulated in the CPC paste. After CPC had set, the degradable microbeads released hUCMSCs inside CPC. hUCMScs proliferated inside CPC, with cell density at 21 d being 4-fold that at 1 d. CPC + 0.1% RGD had the highest cell density, which was 4-fold that of CPC control. The released cells differentiated into the osteogenic lineage and synthesized bone minerals. hUCMSCs inside the CPC + 0.1% RGD construct had gene expressions of alkaline phosphatase (ALP), osteocalcin (OC) and collagen I, which were twice those of CPC control. Mineral synthesis by hUCMSCs inside the CPC + 0.1% RGD construct was 2-fold that in CPC control. RGD and Fn incorporation in CPC did not compromise the strength of CPC, which matched the reported strength of

Correspondence: Dr. Hockin H. K. Xu, Professor, Director of Biomaterials & Tissue Engineering Division, Department of Endodontics, Prosthodontics and Operative Dentistry, University of Maryland Dental School, Baltimore, MD 21201 (hxu@umaryland.edu). Dr. Chongyun Bao, Professor, West China College of Stomatology (cybao9933@yahoo.com.cn).

cancellous bone. In conclusion, degradable microbeads released the hUCMSCs which proliferated, differentiated and synthesized minerals inside the macroporous CPC for the first time. CPC with RGD greatly enhanced cell functions. The novel biofunctionalized and macroporous CPC-microbead-hUCMSC construct is promising for bone tissue engineering applications.

Keywords

Biofunctionalized calcium phosphate cement; human umbilical cord stem cells; gas-foaming porogen; fibronectin; RGD; bone tissue engineering

1. Introduction

Bone defects arise from skeletal diseases, congenital malformations, trauma, and tumor resections [1,2]. Millions of bone fractures occur annually in the United States [3,4]. The need for bone reconstruction is increasing as the population ages. Tissue engineering approaches are promising alternatives to autogenous bone grafts. Studies have shown exciting results on the use of scaffolds and stem cells for tissue regeneration [5–10]. Human umbilical cord mesenchymal stem cells (hUCMSCs) could differentiate into adipocytes, osteoblasts, chondrocytes, neurons, endothelial cells, etc. [11–15]. Umbilical cords provide an inexpensive and inexhaustible stem cell source, without the invasive procedure of bone marrow MSCs, and without the controversies of human embryonic stem cells (hESCs). hUCMSCs appeared to be primitive MSCs with a high plasticity and developmental flexibility, did not cause immunorejection in a preliminary study and were not tumorigenic [14]. Recently, several studies examined hUCMSCs for bone tissue engineering [12,15,16].

Scaffold can serve as a template for cell attachment, differentiation and vascularization *in vivo*, and then can degrade and be replaced by new bone. Calcium phosphate (CaP) scaffolds mimic bone minerals and can bond to bone to form a functional interface [17–20]. Pre-formed CaP implants require machining to fit into a bone cavity. In contrast, calcium phosphate cements can be injected or sculpted, and set *in situ* to form a scaffold with intimate adaptation to neighboring bone [21–25]. They are promising for minimally-invasive surgeries and filling into complex-shaped bone defects. One cement used dicalcium phosphate and tetracalcium phosphate powders, and was referred to as CPC [26,27]. CPC has been shown to possess excellent osteoconductivity and can be replaced by new bone [27].

Recently, CPC composite scaffold was formulated as an injectable carrier for stem cell delivery [16]. The method involves first encapsulating stem cells into hydrogel microbeads, and then mixing the microbeads into the CPC paste. The purpose was to use the microbeads to protect the cells from the paste mixing and injection forces. Once the CPC has set, the microbeads could degrade to release the cells throughout the CPC scaffold, while concomitantly creating macropores in CPC. A recent study showed that CPC containing alginate microbeads was readily injectable, and the encapsulated cells had good viability after injection [16]. However, the alginate microbeads were not degradable and did not release the cells. Therefore, novel alginate-fibrin microbeads were developed that were fast-degradable and could release the encapsulated cells at 4 days [28]. However, that study was performed with the microbeads in the culture well, not inside the CPC scaffold. For the cells inside CPC to survive, the CPC needs to have a high level of macroporosity to enable fluid circulation that provides nutrition and oxygen.

Therefore, the objectives of this study were to: (1) Investigate hUCMSC-encapsulating alginate-fibrin microbeads inside a macroporous CPC construct, and (2) examine cell release

from the microbeads, and cell proliferation and osteogenic differentiation inside CPC. The hypotheses were: (1) The alginate-fibrin microbeads would be able to quickly degrade and release the hUCMSC inside CPC; (2) The released cells inside the macroporous CPC would maintain good viability; (3) Incorporating biofunctional agents into CPC would greatly enhance the released cell attachment to CPC, and enable the cells for osteogenic differentiation and synthesis of bone minerals inside CPC for the first time.

2. Materials and methods

2.1. Fabrication of macroporous and biofunctionalized CPC scaffold

The CPC powder consisted of dicalcium phosphate anhydrous (DCPA: $CaHPO_4$) and tetracalcium phosphate (TTCP: $Ca_4[PO_4]_2O$) mixed at a molar ratio of 1:1. The CPC liquid consisted of chitosan lactate (Vanson, Redmond, WA) mixed with distilled water at a chitosan/(chitosan + water) of 15% mass fraction. Chitosan was used because it could cause fast-setting to the CPC paste and strengthen the CPC [16]. A degradable suture fiber (Vicryl, Ethicon, Somerville, NJ), a copolymer of glycolic and lactic acids, was cut to 3-mm filaments and used at a fiber volume fraction of 20% to reinforce the CPC [16].

A gas-foaming method was used to create macropores in CPC. Following a previous study [29], sodium hydrogen carbonate ($NaHCO_3$) and citric acid monohydrate ($C_6H_8O_7{\cdot}H_2O$) were added into CPC as the porogen. The acid-base reaction of citric acid with $NaHCO_3$ produced CO_2 bubbles in CPC, resulting in macropores. $NaHCO_3$ was added to the CPC powder, at $NaHCO_3$/($NaHCO_3$ + CPC powder) mass fractions of 15%, based on a previous study [30]. That previous study [30] did not investigate biofunctionalized CPC or osteogenic differentiation of hUCMSCs inside CPC. The corresponding amount of $C_6H_8O_7{\cdot}H_2O$ was added to the CPC liquid, to maintain a $NaHCO_3$/($NaHCO_3$ + $C_6H_8O_7{\cdot}H_2O$) mass fraction of 54.52% [29]. This yielded a macroporous CPC scaffold with a pore volume fraction of 73% [30]. This scaffold had no biofunctional agent and is referred to as CPC control.

Two agents known for biofunctionalizing scaffolds and promoting cell adhesion were used: Fibronectin derived from human plasma (Fn, Invitrogen, Carlsbad, CA), and tripeptide Arginyl-Glycyl-Aspartic acid (RGD, Sigma, St. Louis, MO). Fn was dissolved in distilled water. RGD was dissolved in 0.1 mol/L acetic acid. Each biofunctional agent stock solution was mixed with the chitosan liquid, which was then mixed with the CPC powder. To examine the effect of biofunctional agent content in CPC, final Fn mass fractions of 0% (control), 0.05%, and 0.1% were used in CPC. To compare the efficacy of Fn with RGD, RGD in CPC at 0.1% was used. To investigate the combined effect of Fn with RGD, 0.1% Fn + 0.1% RGD was added to CPC.

Therefore, five types of scaffolds were tested: (A) CPC + 0% Fn (CPC control), (B) CPC + 0.05% Fn, (C) CPC + 0.1% Fn, (D) CPC + 0.1% RGD, (E) CPC + 0.1% Fn + 0.1% RGD. CPC powder was mixed with chitosan liquid at a powder:liquid mass ratio of 2:1 [16]. For cell experiments, the paste was placed into a well of a 6-well plate as described in Section 2.3. For mechanical testing, the paste was placed in 3 × 4 × 25 mm molds, incubated at 37 °C for 4 h in a humidor, then demolded and immersed in water at 37 °C for 20 h. Then the specimens were fractured as described in Section 2.7.

2.2 hUCMSC culture

The hUCMSCs (ScienCell, Carlsbad, CA) were harvested from the Wharton's Jelly in umbilical cords of healthy babies [8]. In the present study, hUCMSCs from one donor were used. The use of hUCMSCs was approved by the University of Maryland. hUCMSCs were cultured in a low-glucose Dulbecco's modified Eagle's medium (DMEM) with 10% fetal bovine serum (FBS) and 1% penicillin/streptomycin (Invitrogen, Carlsbad, CA) (control

media). At 80–90% confluence, hUCMSCs were detached by trypsin-EDTA (Invitrogen) and passaged. Passage 4 cells were used. The osteogenic media consisted of the control media supplemented with 100 nM dexamethasone, 10 mM β-glycerophosphate, 0.05 mM ascorbic acid, and 10 nM 1α,25-Dihydroxyvitamin (Sigma).

2.3. hUCMSC encapsulation

Alginate can form an ionically-crosslinked gel under mild conditions without harming the cells, hence alginate microbeads were used to encapsulate cells [16,31]. The cell-encapsulating microbeads were then incorporated into CPC. After the CPC has set, it is desirable for the microbeads to quickly degrade and release the cells, so that the cells can attach to CPC and proliferate inside the scaffold. However, preliminary study showed that the alginate microbeads did not degrade in 4 weeks. Hence, a recent study synthesized oxidized alginate-fibrin microbeads that could quickly release the cells in a few days [28].

Partially oxidizing the alginate enhanced its degradability [32]. The degree of oxidation (%) was the number of oxidized uronate residues per 100 uronate units in the alginate chain. In the present study, the reaction was done at the correct stoichiometric ratio of sodium periodate to alginate to yield 7.5% of alginate oxidation. Following previous studies [28,32], 1% of sodium alginate was dissolved in water. Then, 1.51 mL of 0.25 mol/L sodium periodate (Sigma) was added to 100 mL of alginate solution. After 24 h, the oxidization reaction was stopped by adding 1 g of ethylene glycol and then 2.5 g of sodium chloride. Then, 200 mL of ethanol was added to precipitate the product. The precipitates were re-dissolved in 100 mL of water and precipitated with 200 mL of ethanol. The second precipitates were collected and dissolved in 30 mL of water. The final product was freeze dried for 24 h. This oxidized alginate was dissolved in saline at a concentration of 1.2%. Fibrinogen (Sigma) was added at a concentration of 0.1% and incubated at 37 °C for 2 h to yield the alginate-fibrinogen solution. hUCMSCs were added to this solution at a density of 1 million cells/mL. The solution was filled into a microbead synthesizer (Var J1, Nisco, Switzerland) [16]. Alginate droplets were sprayed into a beaker with 125 mL solution containing 100 mmol/L calcium chloride plus 125 U of thrombin (Sigma). Calcium chloride caused the alginate to crosslink, while the reaction between fibrinogen and thrombin generated the fibrin. This produced oxidized alginate-fibrin microbeads of about 300 μm in sizes [28].

The hUCMSC-encapsulating microbeads were placed inside CPC, as schematically shown in Fig. 1A. First, a layer of CPC paste of 0.3 g was placed on the bottom of a well of a 6-well plate and the surface was made smooth and flat. Then, 0.3 g of microbeads was placed on the CPC surface, and another 0.3 g of CPC paste was used to completely cover the microbeads. The purpose of this setup was to provide a flat bottom surface of CPC, so that the cells released from the microbeads could attach to the flat bottom CPC surface to enable live/dead staining and microscopic analysis. Ideally, the microbeads should be randomly mixed with CPC; however, subsequently breaking the CPC scaffold for analysis would create rough and tortuous surfaces unusable for microscopic examination. In the setup in Fig. 1A, the microbeads were completely wrapped inside CPC, enabling the test of cell survival inside CPC, which relied on the macropores in CPC for access to fluids and nutrition. This enabled the test of whether hUCMSCs inside the macroporous CPC could remain viable and undergo osteogenic differentiation. The freshly placed CPC-microbead construct was incubated at 37 °C for 30 min, then 8 mL of osteogenic media was added to each well to submerge the construct, which was examined as described below. For each experiment at each time point, five constructs were tested for each material (n = 5).

2.4. Viability of hUCMSCs inside macroporous CPC

All of the following cell experiments used the osteogenic media. At culturing for 1, 7, 14 and 21 d, the constructs were carefully opened and gently washed with phosphate buffered saline to remove macroscopic beads or bead remnants, because the focus was the cells on the CPC surface, not the cells inside microbeads. Then, the bottom part of CPC was immersed in a live/dead staining solution (Molecular Probes, Eugene, OR). The bottom surface of CPC as shown in Fig. 1A was examined via epifluorescence microscopy (Eclipse TE-2000S, Nikon, Melville, NY). The percentage of live cells, P, was calculated as: $P = N_L/(N_L + N_D)$, where N_L is the number of live cells, and N_D is the number of dead cells. The live cell density, D, was calculated as: $D = N_L/A$, where A is the area of the view field in which N_L was measured. Three randomly-chosen fields of view were photographed for each specimen. Five specimens (n = 5) yielded 15 photos for each material at each time point.

2.5. Osteogenic differentiation of hUCMSCs inside macroporous CPC

Section 2.4 showed that among the five types of constructs, CPC + 0.1% RGD had the highest live cell density. Therefore, for osteogenic differentiation and mineral synthesis, two types of hUCMSC-encapsulating constructs were tested: CPC control, and CPC + 0.1% RGD. The purpose was to investigate if the cells released from the degradable microbeads inside CPC would be able to undergo osteogenic differentiation, and if RGD incorporation would have a significant effect when compared to CPC control with 0% RGD.

Quantitative real-time reverse transcription polymerase chain reaction (qRT-PCR, 7900HT, Applied Biosystems, Foster City, CA) was used. The total cellular RNA of cells were extracted with TRIzol reagent (Invitrogen) and reverse-transcribed into cDNA using a High-Capacity cDNA Reverse Transcription kit. TaqMan gene expression kits were used to measure the transcript levels of the proposed genes on human alkaline phosphatase (ALP, Hs00758162_m1), osteocalcin (OC, Hs00609452_g1), collagen type I (Coll I, Hs00164004), and glyceraldehyde 3-phosphate dehydrogenase (GAPDH, Hs99999905). Relative expression level for each target gene was evaluated using the $2^{-\Delta\Delta Ct}$ method [16,28]. The C_t values of target genes were normalized by the C_t of the TaqMan human housekeeping gene GAPDH to obtain the ΔC_t values. The C_t of hUCMSCs cultured on tissue culture polystyrene in control media for 1 d served as the calibrator [16,28].

ALP activity was measured using a colorimetric p-nitrophenyl phosphate (pNPP) assay (Stanbio, Boerne, TX) [16]. ALP is an enzyme expressed by cells during osteogenesis and is a well-defined marker for cell differentiation [7,10,12,15,16]. Two types of hUCMSC constructs were tested: CPC control, and CPC + 0.1% RGD. At 1, 7, 14 and 21 d, the cell-encapsulating microbeads were dissolved by 55 mmol/L sodium citrate tribasic solution (Sigma) and lysates were assayed for ALP activity according to the manufacturer's protocol. Control serum (Stanbio) with a known concentration of ALP was used as the standard. A microplate reader (M5 SpectraMax, Molecular Devices, Sunnyvale, CA) was used to measure the absorbance at 405 nm, and the ALP was normalized by the DNA content. DNA was quantified using a Quant-iT PicoGreen Kit (Invitrogen) following standard protocols [16].

2.6. hUCMSCs mineralization inside macroporous CPC

After 1, 7, 14, or 21 d, the constructs were carefully opened, and the flat bottom surface was fixed with 10% formaldehyde and stained with Alizarin Red S (ARS) (Millipore, Billerica, MA). This stained calcium-rich deposits by the cells into a red color. An osteogenesis assay (Millipore) was used to extract the stained minerals and measure the ARS concentration [18]. CPC specimens with the same compositions and same treatment, but without hUCMSCs, were measured as control. The control's ARS concentration was subtracted from

the ARS concentration of the corresponding CPC scaffold with hUCMSCs, to yield the net mineral concentration synthesized by the cells [16,28].

2.7. CPC setting time and flexural testing

CPC setting time was measured using a previous method [33]. The CPC paste was filled into a mold of 3 × 4 × 25 mm and placed in a humidor at 37 °C. At one minute intervals, the specimen was scrubbed gently with figures until the powder component did not come off. This indicated that the setting reaction had occurred sufficiently to hold the specimen together. The time from the powder-liquid mixing to this point was measured as the setting time.

A three-point flexural test was used to fracture the specimens on a Universal Testing Machine (MTS, Eden Prairie, MN) using a span of 20 mm at a crosshead speed of 1 mm/min. Flexural strength was calculated as $S = 3F_{max}L/(2bh^2)$, where F_{max} is the maximum load on the load-displacement (F-d) curve, L is span, b is specimen width and h is thickness. Elastic modulus was calculated as $E = (F/d)\ (L^3/[4bh^3])$.

2.8. Scanning electron microscopy and statistical analysis

A scanning electron microscope (SEM, JEOL 5300, Peabody, MA) was used to examine the hUCMSC attachment on the bottom surfaces of CPC. Specimens with cells cultured for 7 d were fixed with 1% glutaraldehyde, subjected to graded alcohol dehydrations, rinsed with hexamethyldisilazane, sputter coated with gold, and examined in SEM.

One-way and two-way ANOVA were performed to detect significant ($\alpha = 0.05$) effects of the variables. Tukey's multiple comparison procedures were used to group and rank the measured values at a family confidence coefficient of 0.95.

3. Results

The schematic of CPC construct containing hUCMSC-encapsulating microbeads is shown in Fig. 1A. Figs. 1B and 1C are optical photos of hUCMSC-encapsulating alginate-fibrin microbeads cultured for 1 d and 7 d. At 1 d, the microbead was intact and not degraded, and the encapsulated cells had a round shape. At 7 d, the microbeads degraded and the cells were released, which showed an elongated or spreading morphology.

Live/dead images of the bottom surface of CPC are shown in Fig. 2A–J. There was an increase in cell number from 1 d to 21 d. CPC + 0.1% RGD had the most cells. The effect of biofunctional agents was shown more clearly at a higher magnification in (K) for CPC control, and (L) for CPC + 0.1% RGD. The cells appeared as round dots in (K) because they were encapsulated in the microbeads. The spreading cells in (L) indicate that they were released and attached to the surface of CPC + 0.1% RGD. Some cells near the surface of the microbeads migrated out of the microbeads and onto the CPC surface by 1 d. The number of spreading cells increased with increasing time from 1 to 21 d. Among the different constructs, CPC with Fn and RGD had more attaching cells than CPC control, and CPC with 0.1% RGD had the most amount of attaching cells. At 7 d, microbead remnants were present on the CPC surfaces. At 14 d, there were much less microbead remnants. At 21 d, very few microbead remnants could be found, and only small amounts of fine pieces of microbead remnants could be found in the CPC surfaces under the microscope. SEM examination verified that cells attached to CPC. A representative example in (M) for CPC + 0.1% RGD showed that the cell adhered to CPC and developed cytoplasmic extensions (arrows).

Fig. 3 plots (A) the percentage of live cells, and (B) live cell density (mean ± sd; n = 5). CPC with 0.1% Fn had a higher cell density than that with 0.05% Fn ($p < 0.05$). CPC +

0.1% RGD had the highest cell density. For CPC + 0.1% RGD, the cell density increased by 4-fold from 1 to 21 d due to proliferation. At 21 d, the cell density on CPC + 0.1% RGD was about 4 times that of CPC control.

The RT-PCR results for hUCMSCs released from the microbeads and attached to CPC are plotted in Fig. 4. hUCMSCs inside CPC showed osteogenic differentiation, indicated by ALP, OC and collagen I exhibiting peak gene expressions, which were much higher than the 1 d expressions (mean ± sd; n = 5). For each marker, CPC biofunctionalized with RGD had higher peaks than that for CPC control ($p < 0.05$). These data demonstrate that adding RGD increased the osteogenic gene expressions of the hUCMSCs inside the CPC scaffold.

The synthesis of ALP protein by hUCMSCs inside the macroporous CPC was measured. The ALP activity is plotted in Fig. 5 (mean ± sd; n = 5). ALP protein synthesis peaked at 14 d for CPC control and CPC + 0.1% RGD. The ALP peak for CPC + 0.1% RGD was twice as high as that of CPC control ($p < 0.01$). Regarding culture time, the ALP activity at 14 d was 18-fold of that at 1 d for CPC + 0.1% RGD.

Mineral synthesis by hUCMSCs inside the constructs is shown in Fig. 6. ARS staining of CPC showed a red color. In (A) to (F), there was a dark red staining of minerals synthesized by the cells, which accumulated on CPC. The mineral staining was thicker and denser on CPC + 0.1% RGD than that on CPC control. A layer of matrix mineralization by the cells covered the entire bottom surface of CPC + 0.1% RGD at 21 d. Data from the osteogenesis assay are plotted in (G) (mean ± sd; n = 5). At 21 d, the mineral amount on CPC + 0.1% RGD was 2-fold that on CPC control. Hence, hUCMSCs inside CPC differentiated into the osteogenic lineage and mineral synthesis was increased via RGD.

Fig. 7 shows that adding RGD and Fn to biofunctionalize the CPC did not compromise the setting time and mechanical properties of CPC (mean ± sd; n = 6). The gas-foaming macroporous CPC with 0.1% RGD had a setting time of (12.3 ± 0.3) min, a flexural strength of (4.2 ± 0.7) MPa, and an elastic modulus of (820 ± 110) MPa.

4. Discussion

CPC is a promising carrier for injectable delivery of stem cells and growth factors in moderate load-bearing areas for bone regeneration. The injectability of CPC containing cell-encapsulating microbeads and fibers was shown in a previous study [16]. The microbeads protected the cells from the paste mixing and injection forces, with cell viability after injection being similar to that before injection. The CPC paste can form intimate adaptation to complex-shaped bone defects and bond to neighboring bone to form a functional interface. The good mechanical properties as shown in the present study could enable stem cell delivery in moderate load-bearing repairs. For example, in mandibular and maxillary ridge augmentation, CPC could be molded to the desired shape for esthetics, and then set to form a macroporous scaffold containing stem cells for bone regeneration. These implants would be subjected to early loading by provisional dentures. Therefore, the macroporous CPC scaffold needs to be resistant to flexure. In addition, the CPC paste could be used in major reconstructions of the maxilla or mandible after trauma or tumor resections, which would require the CPC to be fracture resistant. CPC could also be used in the support of metal dental implants or augmentation of deficient implant sites where mechanical properties are important. It should be noted that to repair large defects, mechanical strength is only one factor to consider. Other factors such as vascularization are also critically important for success [34,35], and further study should investigate the incorporation of endothelial cells and growth factors into CPC scaffold to promote angiogenesis. The macroporous CPC of the present study possessed better mechanical properties than other injectable carriers for cell delivery. For example, previous studies reported that an injectable

polymeric carrier for cell delivery had a strength of 0.7 MPa [36], and hydrogels had strengths of about 0.1 MPa [37,38]. These systems are promise for non-load-bearing applications. However, their strengths are much lower than the reported strength of about 3.5 MPa for cancellous bone [39]. The macroporous CPC + 0.1% RGD with a strength of 4.2 MPa matched that of cancellous bone, and hence may be a promising injectable scaffold for stem cell encapsulation in orthopedic and craniofacial applications.

Stem cell encapsulation and delivery in CPC has three main challenges. First, the CPC needs to be macroporous to provide fluid circulation and nutrition to the cells in the scaffold. In a previous study [30], in CPC without the gas-foaming porogen, the percentage of live cells was only 49%. In contrast, with the incorporation of 15% gas-foaming porogen in CPC, the percentage of live cells was increased to 85%. This resulted from the increase in pore volume fraction from the intrinsic porosity of 47% for CPC without additional porogen, to 73% for CPC by adding porogen [30]. That previous study did not investigate osteogenic differentiation inside CPC or the functionalization of CPC via Fn and RGD.

The second challenge is for the microbeads inside CPC to quickly degrade to release the cells inside CPC. The initial setting of CPC takes several minutes, and the complete setting reaction takes about a day. After the CPC has set, it is desirable for the microbeads to quickly degrade and release the cells, so that the cells can attach to CPC and proliferate, while the microbead degradation creates additional macropores in CPC. However, alginate hydrogels take weeks to months to degrade. In a previous study [28], alginate microbeads with 7.5% oxidation were still intact after 21 d. However, the addition of a small amount of fibrin dramatically increased the microbead degradation. The alginate-fibrin microbeads degraded and released the cells starting at 4 d [28]. That study was performed with microbeads on tissue culture polystyrene, and not encapsulated inside CPC.

The third challenge is that the cells released from the microbeads need to attach to CPC and be able to proliferate. Cell attachment is an important regulator of many cellular functions, such as viability, proliferation, migration, and differentiation. However, preliminary study showed that the released cell attachment inside CPC was relatively poor. This is consistent with previous studies showing that human stem cell attachment to CPC was relatively poor [40,41]. Therefore, there is a need to improve cell attachment to CPC.

The present study addressed these three challenges. The following results were achieved for the first time: (1) The alginate-fibrin microbeads quickly released the hUCMSCs inside CPC; (2) the released cells maintained good viability inside the gas-foaming microporous CPC; (3) functionalization of CPC via Fn and RGD greatly enhanced the attachment and proliferation of the released hUCMSCs inside CPC; (4) the released hUCMSCs differentiated down the osteogenic lineage and synthesized bone minerals. For CPC with Fn and RGD, microscopic examination of live/dead stained CPC surfaces revealed mostly cells with a spreading morphology at 7–21 d, indicating that they were released from the microbeads and attached to CPC. The majority of the microbeads had degraded and the majority of the encapsulated cells had been released by 14 and 21 d. In Fig. 3B, for CPC with RGD and Fn from 7 to 21 d, the majority of the cells in the live cell density measurement were cells with a spreading morphology. This indicates that these were cells released from the microbeads and attached to the surface of the CPC scaffold, which was confirmed by SEM observations. Macroporous CPC using gas-foaming porogen provided media access to the cells inside the scaffold, manifested by good cell viability and fast proliferation. The microbeads inside CPC degraded within 7 d and released the cells to attach to CPC. Cells inside the hydrogel showed as round dots, with no spreading and no proliferation. In contrast, the cells released from the microbeads attached to CPC, showed a healthy spreading morphology, and quickly proliferated. Furthermore, in previous studies,

Fn and RGD were used to promote cell adhesion to biomaterials including pre-formed calcium phosphates [42,43]. However, there has been no report on incorporating Fn and RGD into CPC.

Fn, a member of the family of adhesive matrix glycoproteins, is a major component of the extracellular matrix (ECM) and plays a key role in cell adhesion, growth, migration and differentiation [44–47]. The Fn molecule consists of repeating globular domains with specific cell-binding sites for interactions with transmembrane receptor proteins called integrin. In addition to integrin, Fn also binds to ECM components such as collagen, fibrin and heparan sulfate proteoglycans. Fn improved cell spreading, attachment and proliferation on many biomaterials, including ceramics, bioactive glasses, polymers and hydrogels [44–47]. In the present study, a larger number of hUCMSCs spread out and attached to CPC + 0.1% Fn, than CPC + 0.05% Fn and CPC control. Therefore, Fn enhanced the cell adhesion to the CPC, whereas cells could float away from the CPC surface if Fn was not present.

Another approach is to present cells with recognition motifs such as small immobilized peptides [48]. RGD, a tripeptide originally identified as the sequence within Fn that mediates cell attachment, has been found in numerous other proteins. RGD has a widespread distribution throughout the organism, the ability to address many cell adhesion receptors, and a strong impact on cell anchoring, behavior and survival. As a result, RGD is by far the most effective and most frequently-used peptide sequence to stimulate cell adhesion. Indeed, RGD has been applied on many biomaterials such as glass, polymers and ceramics to improve cell adhesion [49–54].

The present study showed that CPC biofunctionalized with RGD greatly enhanced hUCMSC attachment and proliferation inside CPC. Many cells in CPC + 0.1% RGD at 1 d showed a healthy spreading morphology (Fig. 2L), while cells in CPC control remained as green dots (Fig. 2K). A previous study demonstrated that it took 4 d for the microbeads to significantly degrade [28]. Therefore, the cell attachment and spreading on CPC in Fig. 2L was not due to microbead degradation. Instead, it was likely because that, for the microbeads on the bottom surface of CPC + 0.1% RGD, the cells in the microbeads near the bottom surface migrated out of the microbeads and attached to CPC with RGD. Our preliminary study indicated that the cells liked to migrate toward an area that contained RGD. For example, in preliminary study, RGD was incorporated into the microbeads; however, this hindered the cell release from the microbeads, as the cells stayed inside the microbeads where the RGD was present. Furthermore, the present study showed that CPC biofunctionalized with RGD was more effective than CPC with Fn in promoting a spreading cell morphology and cell proliferation. Interestingly, the CPC + 0.1% Fn + 0.1% RGD construct had a lower cell density than that of CPC + 0.1% RGD. A previous study suggested that there were interactions between Fn and RGD that inhibited cell attachment to hydroxyapatite [55]. This is because the potency of RGD could be affected by its steric conformation and surrounding sequences [56]. The binding between RGD and its ligands, the integrin on cell surfaces, is similar to the relationship between the key and the lock. Therefore, when the conformation of RGD changed, the activity of RGD decreased. In the present study, the finding that there was less cell adhesion to the Fn + RGD construct than to the RGD construct, suggests that there were likely interactions between Fn and RGD that affected their steric conformations and reduced cell attachment. Further study is needed to investigate this issue.

hUCMSCs released from the microbeads inside CPC differentiated into the osteogenic lineage. Previous studies showed that gene expressions of ALP, OC, and Coll I played key roles in the osteogenic differentiation of MSCs [10,12,57,58]. As an enzyme expressed by MSCs during osteogenesis, ALP is a well-defined marker for differentiation. During

osteogenic differentiation of the MSCs, the gene expression of ALP is first upregulated at the early stage of osteogenic differentiation. Then, as the cascade of events for the differentiation continues, other markers such as OC and Coll I become upregulated, while the ALP is decreased [16,59]. This is consistent with the present study showing that ALP peaked earlier than OC and Coll I. In addition, the present study showed higher osteogenic gene expressions for CPC with RGD than that without RGD. Regarding the mechanism for RGD-driven enhancement of osteogenesis, the RGD used in the present study was soluble in 0.1 mol/L acetic acid but insoluble in water. Hence, the RGD stock solution was prepared with 0.1 mol/L acetic acid and then mixed into CPC. After the CPC had set, RGD was distributed throughout the CPC scaffold volume including the surface. The majority of the RGD likely remained in the CPC and did not dissolve into the culture media because the RGD was insoluble in water. The ligation between the cell integrin and the RGD on the CPC surface was likely responsible for the enhanced cell attachment to CPC. This in turn could activate certain signaling pathways and increase the osteogenesis. The mechanism of RGD enhancing osteogenesis is interesting and requires further investigation. Our observation that RGD promoted osteogenic gene expression is consistent with previous studies using different substrates and cells [60,61]. The higher bone markers for CPC + 0.1% RGD were consistent with the mineral results, which showed that hUCMSCs in CPC + 0.1% RGD synthesized twice as much mineral as that in CPC without RGD. These results show that the gas-foaming CPC paste with alginate-fibrin microbeads could be a promising system to deliver stem cells, and RGD incorporation into CPC could greatly enhance the function hUCMSCs inside CPC. The present study used hUCMSCs from one donor. Further study should use hUCMSCs from several different donors and investigate the effects of different donors on cell proliferation and osteogenic differentiation for bone tissue engineering. Further study is also needed to evaluate the hUCMSC-encapsulating macroporous CPC-RGD construct for bone regeneration in an animal model.

5. Conclusion

This study developed a biofunctionalized and macroporous CPC with excellent stem cell proliferation, osteogenic differentiation and bone mineral synthesis inside CPC for the first time. The novel alginate-fibrin microbeads degraded quickly and released the cells inside CPC to attach to CPC. hUCMSCs maintained good viability inside the macroporous CPC. Incorporation of Fn and RGD into CPC greatly enhanced cell attachment, with RGD yielding the highest cell density, which was 4-fold that of CPC control. Osteogenic differentiation was enhanced via RGD in CPC, exhibiting high gene expressions of ALP, OC and collagen I, as well as a high ALP activity. hUCMSCs inside CPC synthesized bone minerals, and cell mineralization was doubled via RGD in CPC. Mechanical strength of macroporous CPC was not degraded with RGD addition, and matched the reported strength of cancellous bone. In conclusion, the macroporous and biofunctionalized CPC was a promising carrier for stem cell delivery, and the alginate-fibrin microbeads could protect the cells and then quickly release the cells inside CPC. The novel CPC-RGD-microbead construct with hUCMSC encapsulation greatly enhanced cell proliferation, differentiation and mineral synthesis, and hence is promising for orthopedic and craniofacial applications.

Acknowledgments

We thank the technical support of the Core Imaging Facility of the University of Maryland, Drs. L. C. Chow at the Paffenbarger Research Center, and Dr. Carl G. Simon at the National Institute of Standards and Technology for discussions. We thank Prof. Xuedong Zhou and Prof. Qianming Chen of the West China College of Stomatology for support. This study was supported by NIH R01 grants DE14190 and DE17974 (HX), Maryland Stem Cell Fund (HX), University of Maryland School of Dentistry, and West China College of Stomatology.

References

1. Mao, JJ.; Vunjak-Novakovic, G.; Mikos, AG.; Atala, A. Regenerative medicine: Translational approaches and tissue engineering. Vol. Chapters 1–3. Boston, MA: Artech House; 2007.
2. Bohner M. Design of ceramic-based cements and putties for bone graft substitution. Eur Cell Mater. 2010; 20:1–12. [PubMed: 20574942]
3. The burden of musculoskeletal conditions at the start of the new millennium. Geneva, Switzerland: WHO; 2003. WHO Technical Report Series 919; p. 102-103.
4. Salgado AJ, Coutinho OP, Reis RL. Bone tissue engineering: state of the art and future trends. Macromol Biosci. 2004; 4:743–765. [PubMed: 15468269]
5. Bohner M, Baroud G. Injectability of calcium phosphate pastes. Biomaterials. 2005; 26:1553–1563. [PubMed: 15522757]
6. Ginebra MP, Traykova T, Planell JA. Calcium phosphate cements as bone drug-delivery systems: a review. J Controlled Release. 2006; 113:102–110.
7. Benoit DS, Nuttelman CR, Collins SD, Anseth KS. Synthesis and characterization of a fluvastatin-releasing hydrogel delivery system to modulate hMSC differentiation and function for bone regeneration. Biomaterials. 2006; 27:6102–10. [PubMed: 16860387]
8. Mao JJ, Giannobile WV, Helms JA, Hollister SJ, Krebsbach PH, Longaker MT. Craniofacial tissue engineering by stem cells. J Dent Res. 2006; 85:966–979. [PubMed: 17062735]
9. Johnson PC, Mikos AG, Fisher JP, Jansen JA. Strategic directions in tissue engineering. Tissue Eng. 2007; 13:2827–37. [PubMed: 18052823]
10. Habibovic P, Gbureck U, Doillon CJ, Bassett DC, van Blitterswijk CA, Barralet JE. Osteoconduction and osteoinduction of low-temperature 3D printed bioceramic implants. Biomaterials. 2008; 29:944–953. [PubMed: 18055009]
11. Wang HS, Hung SC, Peng ST, Huang CC, Wei HM, Guo YJ, et al. Mesenchymal stem cells in the Wharton's jelly of the human umbilical cord. Stem Cells. 2004; 22:1330–7. [PubMed: 15579650]
12. Baksh D, Yao R, Tuan RS. Comparison of proliferative and multilineage differentiation potential of human mesenchymal stem cells derived from umbilical cord and bone marrow. Stem Cells. 2007; 25:1384–92. [PubMed: 17332507]
13. Bailey MM, Wang L, Bode CJ, Mitchell KE, Detamore MS. A comparison of human umbilical cord matrix stem cells and temporomandibular joint condylar chondrocytes for tissue engineering temporomandibular joint condylar cartilage. Tissue Eng. 2007; 13:2003–10. [PubMed: 17518722]
14. Can A, Karahuseyinoglu S. Concise review: human umbilical cord stroma with regard to the source of fetus-derived stem cells. Stem Cells. 2007; 25:2886–95. [PubMed: 17690177]
15. Wang L, Singh M, Bonewald LF, Detamore MS. Signalling strategies for osteogenic differentiation of human umbilical cord mesenchymal stromal cells for 3D bone tissue engineering. J Tissue Eng Regen Med. 2009; 3:398–404. [PubMed: 19434662]
16. Zhao L, Weir MD, Xu HHK. An injectable calcium phosphate-alginate hydrogel-umbilical cord mesenchymal stem cell paste for bone tissue engineering. Biomaterials. 2010; 31:6502–10. [PubMed: 20570346]
17. Foppiano S, Marshall SJ, Marshall GW, Saiz E, Tomsia AP. The influence of novel bioactive glasses on in vitro osteoblast behavior. J Biomed Mater Res A. 2004; 71:242–249. [PubMed: 15372470]
18. Deville S, Saiz E, Nalla RK, Tomsia AP. Freezing as a path to build complex composites. Science. 2006; 311:515–518. [PubMed: 16439659]
19. Reilly GC, Radin S, Chen AT, Ducheyne P. Differential alkaline phosphatase responses of rat and human bone marrow derived mesenchymal stem cells to 45S5 bioactive glass. Biomaterials. 2007; 28:4091–4097. [PubMed: 17586040]
20. Kasten P, Beyen I, Niemeyer P, Luginbuhl R, Bohner M, Richter W. Porosity and pore size of beta-tricalcium phosphate scaffold can influence protein production and osteogenic differentiation of human mesenchymal stem cells: an in vitro and in vivo study. Acta Biomater. 2008; 4:1904–15. [PubMed: 18571999]

21. Ginebra MP, Rilliard A, Fernández E, Elvira C, Román JS, Planell JA. Mechanical and rheological improvement of a calcium phosphate cement by the addition of a polymeric drug. J Biomed Mater Res. 2001; 57:113–118. [PubMed: 11416857]
22. Barralet JE, Gaunt T, Wright AJ, Gibson IR, Knowles JC. Effect of porosity reduction by compaction on compressive strength and microstructure of calcium phosphate cement. J Biomed Mater Res B. 2002; 63:1–9.
23. Ginebra MP, Driessens FC, Planell JA. Effect of the particle size on the micro and nanostructural features of a calcium phosphate cement: a kinetic analysis. Biomaterials. 2004; 25:3453–62. [PubMed: 15020119]
24. Bohner M, Gbureck U, Barralet JE. Technological issues for the development of more efficient calcium phosphate bone cements: a critical assessment. Biomaterials. 2005; 26:6423–9. [PubMed: 15964620]
25. Jansen JA, Vehof JW, Ruhe PQ, Kroeze-Deutman H, Kuboki Y, Takita H, et al. Growth factor-loaded scaffolds for bone engineering. J Control Release. 2005; 101:127–36. [PubMed: 15588899]
26. Brown, WE.; Chow, LC. A new calcium phosphate water setting cement. In: Brown, PW., editor. Cements research progress. Westerville, OH: Am Ceram Soc; 1986. p. 352-379.
27. Friedman CD, Costantino PD, Takagi S, Chow LC. BoneSource hydroxyapatite cement: a novel biomaterial for craniofacial skeletal tissue engineering and reconstruction. J Biomed Mater Res. 1998; 43:428–432. [PubMed: 9855201]
28. Zhou H, Xu HHK. The fast release of stem cells from alginate-fibrin microbeads in injectable scaffolds for bone tissue engineering. Biomaterials. 2011; 32:7503–7513. [PubMed: 21757229]
29. Hesaraki S, Zamanian A, Moztarzadeh F. The influence of the acidic component of the gas-foaming porogen used in preparing an injectable porous calcium phosphate cement on its properties: acetic acid versus citric acid. J Biomed Mater Res B. 2008; 86:208–16.
30. Chen WC, Zhou HZ, Tang MH, Weir MD, Bao CY, Xu HHK. Gas-foaming calcium phosphate cement scaffold encapsulating human umbilical cord stem cells. Tissue Eng Part A. (in press).
31. Weir MD, Xu HHK, Simon CG. Strong calcium phosphate cement-chitosan-mesh construct containing cell-encapsulating hydrogel beads for bone tissue engineering. J Biomed Mater Res A. 2006; 77:487–96. [PubMed: 16482548]
32. Bouhadir KH, Lee KY, Alsberg E, Damm KL, Anderson KW, Mooney DJ. Degradation of partially oxidized alginate and its potential application for tissue engineering. Biotechnol Prog. 2001; 17:945–950. [PubMed: 11587588]
33. Xu HHK, Takagi S, Quinn JB, Chow LC. Fast-setting calcium phosphate scaffolds with tailored macropore formation rates for bone regeneration. J Biomed Mater Res A. 2004; 68:725–34. [PubMed: 14986327]
34. Rouwkema J, Rivron NC, van Blitterswijk CA. Vascularization in tissue engineering. Trends Biotechnol. 2008; 26:434–41. [PubMed: 18585808]
35. Lovett M, Lee K, Edwards A, Kaplan DL. Vascularization strategies for tissue engineering. Tissue Eng Part B Rev. 2009; 15:353–70. [PubMed: 19496677]
36. Shi X, Sitharaman B, Pham QP, Liang F, Wu K, Edward BW, et al. Fabrication of porous ultra-short single-walled carbon nanotube nanocomposite scaffolds for bone tissue engineering. Biomaterials. 2007; 28:4078–4090. [PubMed: 17576009]
37. Kuo CK, Ma PX. Ionically crosslinked alginate hydrogels as scaffolds for tissue engineering: part 1. Structure, gelation rate and mechanical properties. Biomaterials. 2001; 22:511–21. [PubMed: 11219714]
38. Drury JL, Dennis RG, Mooney DJ. The tensile properties of alginate hydrogels. Biomaterials. 2004; 25:3187–99. [PubMed: 14980414]
39. Damien CJ, Parsons JR. Bone graft and bone graft substitutes: a review of current technology and applications. J Appl Biomater. 1991; 2:187–208. [PubMed: 10149083]
40. Link DP, den Dolder J, Wolke JG, Jansen JA. The cytocompatibility and early osteogenic characteristics of an injectable calcium phosphate cement. Tissue Eng. 2007; 13:493–500. [PubMed: 17362133]
41. Weir MD, Xu HHK. Culture human mesenchymal stem cells with calcium phosphate cement scaffolds for bone repair. J Biomed Mater Res B. 2010; 93:93–105.

42. Sogo Y, Ito A, Matsuno T, Oyane A, Tamazawa G, Satoh T, et al. Fibronectin-calcium phosphate composite layer on hydroxyapatite to enhance adhesion, cell spread and osteogenic differentiation of human mesenchymal stem cells in vitro. Biomed Mater. 2007; 2:116–23. [PubMed: 18458444]
43. Schneiders W, Reinstorf A, Pompe W, Grass R, Biewener A, Holch M, et al. Effect of modification of hydroxyapatite/collagen composites with sodium citrate, phosphoserine, phosphoserine/RGD-peptide and calcium carbonate on bone remodelling. Bone. 2007; 40:1048–59. [PubMed: 17223400]
44. Nuttelman CR, Mortisen DJ, Henry SM, Anseth KS. Attachment of fibronectin to poly(vinyl alcohol) hydrogels promotes NIH3T3 cell adhesion, proliferation, and migration. J Biomed Mater Res. 2001; 57:217–223. [PubMed: 11484184]
45. Schonmeyr BH, Wong AK, Li S, Gewalli F, Cordiero PG, Mehrara BJ. Treatment of hydroxyapatite scaffolds with fibronectin and fetal calf serum increases osteoblast adhesion and proliferation in vitro. Plast Reconstr Surg. 2008; 121:751–62. [PubMed: 18317125]
46. Custodio CA, Alves CM, Reis RL, Mano JF. Immobilization of fibronectin in chitosan substrates improves cell adhesion and proliferation. J Tissue Eng Regen Med. 2010; 4:316–23. [PubMed: 20049746]
47. Martyn SV, Heywood HK, Rockett P, Paine MD, Wang MJ, Dobson PJ, et al. Electrospray deposited fibronectin retains the ability to promote cell adhesion. J Biomed Mater Res B. 2011; 96:110–8.
48. Hersel U, Dahmen C, Kessler H. RGD modified polymers: biomaterials for stimulated cell adhesion and beyond. Biomaterials. 2003; 24:4385–415. [PubMed: 12922151]
49. Massia SP, Hubbell JA. Covalent surface immobilization of Arg-Gly-Asp- and Tyr-Ile-Gly-Ser-Arg-containing peptides to obtain well-defined cell-adhesive substrates. Anal Biochem. 1990; 187:292–301. [PubMed: 2382830]
50. Hu Y, Winn SR, Krajbich I, Hollinger JO. Porous polymer scaffolds surface-modified with arginine-glycine-aspartic acid enhance bone cell attachment and differentiation in vitro. J Biomed Mater Res A. 2003; 64:583–590. [PubMed: 12579573]
51. Durrieu MC, Pallu S, Guillemot F, Bareille R, Amedee J, Baquey CH, et al. Grafting RGD containing peptides onto hydroxyapatite to promote osteoblastic cells adhesion. J Mater Sci Mater Med. 2004; 15:779–86. [PubMed: 15446238]
52. Huang Y, Ren J, Ren T, Gu S, Tan Q, Zhang L, et al. Bone marrow stromal cells cultured on poly (lactide-co-glycolide)/nano-hydroxyapatite composites with chemical immobilization of Arg-Gly-Asp peptide and preliminary bone regeneration of mandibular defect thereof. J Biomed Mater Res A. 2010; 95:993–1003. [PubMed: 20872750]
53. Zhang P, Wu H, Wu H, Lu Z, Deng C, Hong Z, Jing X, Chen X. RGD-conjugated copolymer incorporated into composite of poly(lactide-co-glycotide) and poly(L-lactide)-grafted nanohydroxyapatite for bone tissue engineering. Biomacromolecules. 2011; 12:2667–80. [PubMed: 21604718]
54. Huang Y, Luo Q, Li X, Zhang F, Zhao S. Fabrication and in vitro evaluation of the collagen/hyaluronic acid PEM coating crosslinked with functionalized RGD peptide on titanium. Acta Biomater. 2012; 8:866–77. [PubMed: 22040683]
55. Sawyer AA, Hennessy KM, Bellis SL. Regulation of mesenchymal stem cell attachment and spreading on hydroxyapatite by RGD peptides and adsorbed serum proteins. Biomaterials. 2005; 26:1467–75. [PubMed: 15522748]
56. Schaffner P, Dard MM. Structure and function of RGD peptides involved in bone biology. Cell Mol Life Sci. 2003; 60:119–32. [PubMed: 12613662]
57. Datta N, Holtorf HL, Sikavitsas VI, Jansen JA, Mikos AG. Effect of bone extracellular matrix synthesized in vitro on the osteoblastic differentiation of marrow stromal cells. Biomaterials. 2005; 26:971–977. [PubMed: 15369685]
58. Chatterjee K, Lin-Gibson S, Wallace WE, Parekh SH, Lee YJ, Cicerone MT, et al. The effect of 3D hydrogel scaffold modulus on osteoblast differentiation and mineralization revealed by combinatorial screening. Biomaterials. 2010; 31:5051–5062. [PubMed: 20378163]

59. Kim K, Dean D, Mikos AG, Fisher JP. Effect of initial cell seeding density on early osteogenic signal expression of rat bone marrow stromal cells cultured on cross-linked poly(propylene fumarate) disks. Biomacromolecules. 2009; 10:1810–1817. [PubMed: 19469498]

60. Yang F, Williams CG, Wang DA, Lee H, Manson PN, Elisseeff J. The effect of incorporating RGD adhesive peptide in polyethylene glycol diacrylate hydrogel on osteogenesis of bone marrow stromal cells. Biomaterials. 2005; 26:5991–5998. [PubMed: 15878198]

61. Morgan AW, Roskov KE, Lin-Gibson S, Kaplan DL, Becker ML, Simon CG. Characterization and optimization of RGD-containing silk blends to support osteoblastic differentiation. Biomaterials. 2008; 29:2556–2563. [PubMed: 18325585]

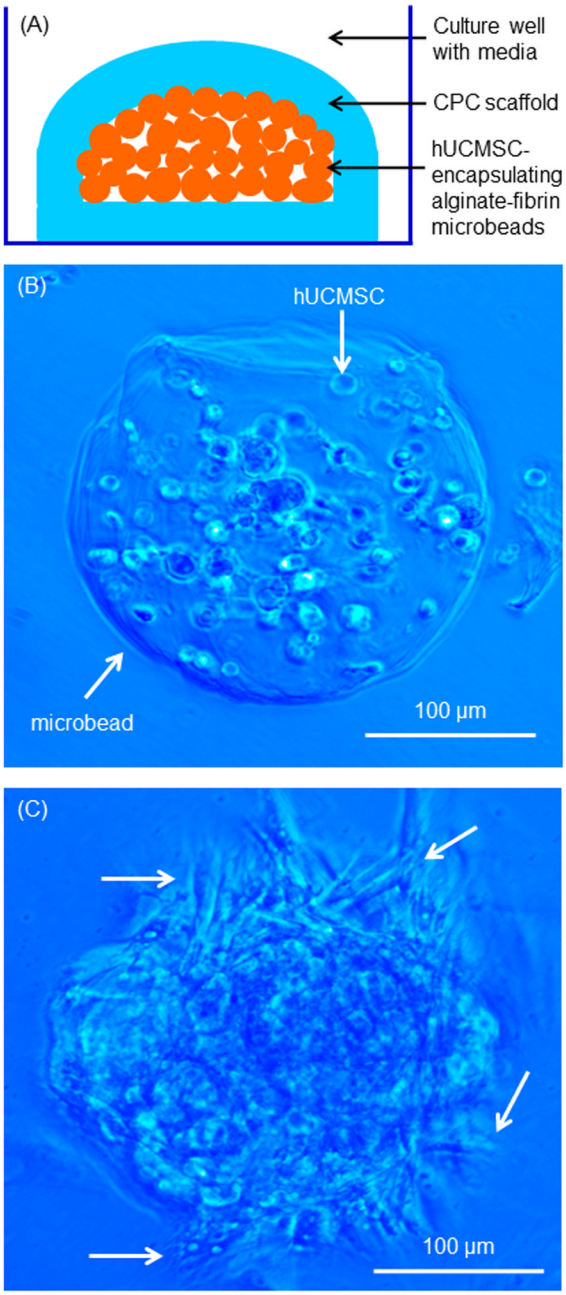

Fig. 1.

hUCMSC-encapsulating microbeads in CPC. (A) Schematic of microbeads inside CPC. (B, C) Optical photos of hUCMSC-encapsulating microbeads at 1 d and 7 d. A blue filter was used to enhance the contrast of the microbeads. Arrows in B indicate that at 1 d, the microbead was intact and not degraded, and the encapsulated cells appeared as round dots. Arrows in C indicate that at 7 d, the cells were released from the degrading microbeads and had an elongated or spreading morphology.

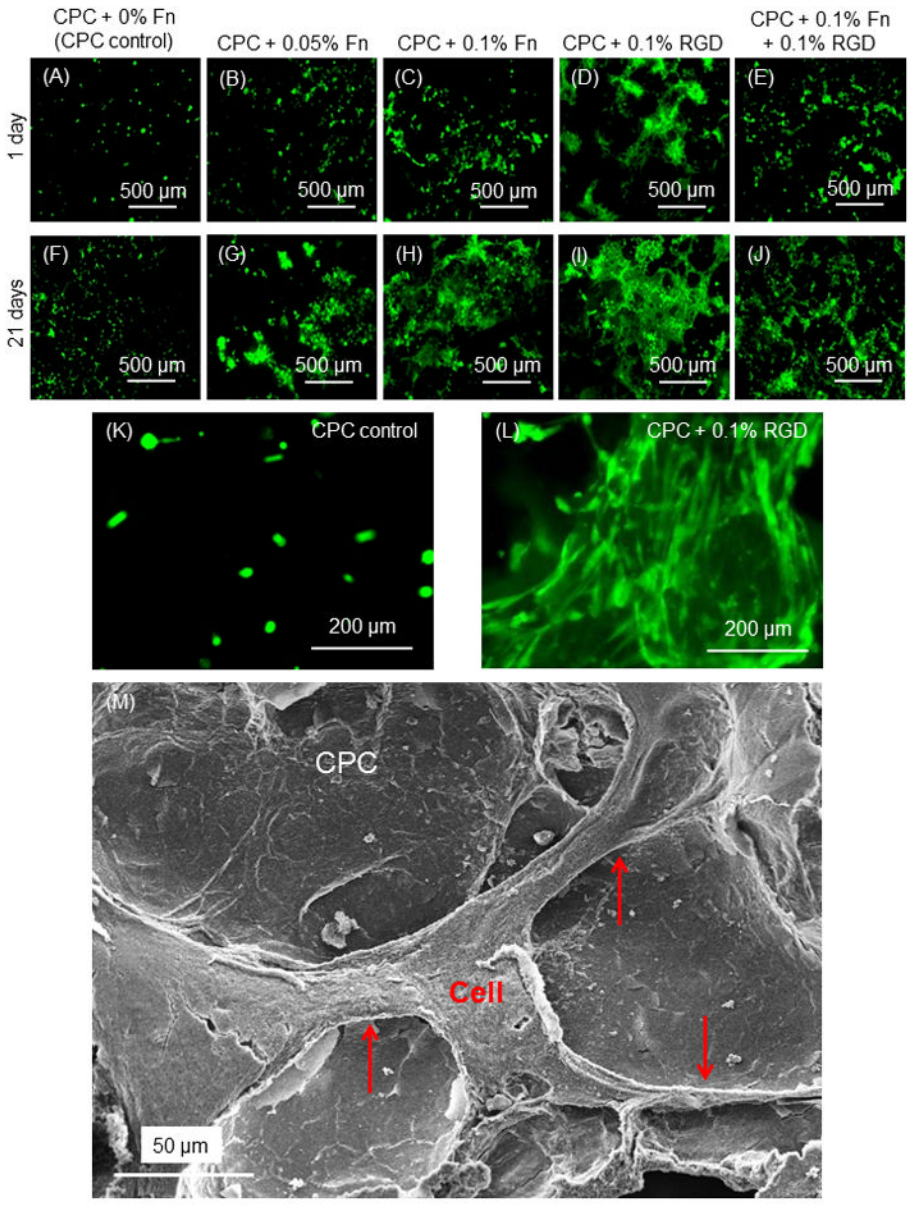

Fig. 2.

Live/dead staining. (A–L) Live cells were stained green and were numerous. Dead cells were stained red and were very few (not included). There was an increase in cell numbers from 1 d to 21 d, with CPC + 0.1% RGD having the most cells. (K–L) Higher magnification in (K) for CPC control at 1 d, and (L) for CPC + 0.1% RGD at 1 d, showing improved cell attachment with a spreading morphology due to RGD in CPC. (M) Representative SEM image attaching to the bottom surface of CPC + 0.1% RGD with long cytoplasmic extensions (arrows). This example was cultured for 7 d. Other culture times had similar cell attachment and cytoplasmic extensions.

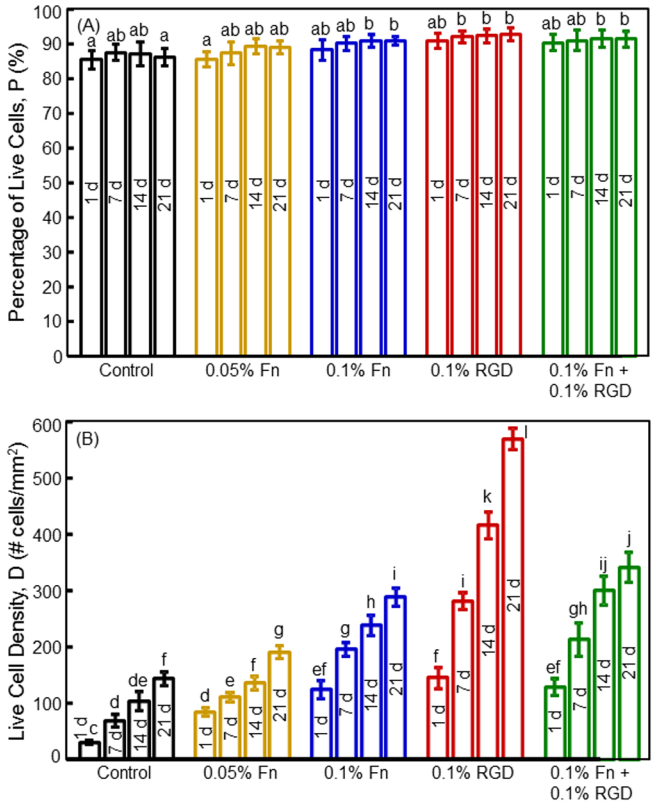

Fig. 3.

Viability and proliferation of hUCMSCs released from microbeads inside CPC scaffolds: (A) Percentage of live cells, and (B) live cell density. Each value is mean ± sd; n = 5. Values with dissimilar letters are significantly different ($p < 0.05$).

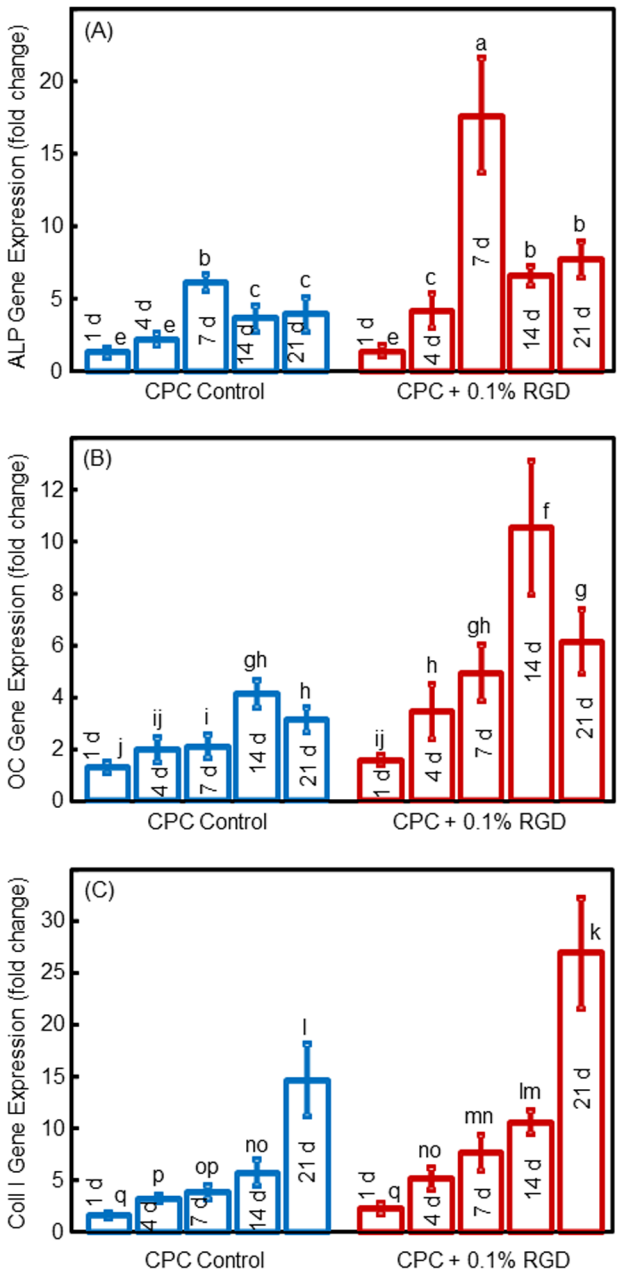

Fig. 4.

RT-PCR results for osteogenic differentiation of the released hUCMSCs: (A) ALP, (B) OC, and (C) Collagen I gene expressions. Each value is mean ± sd; n = 5. In each plot, values with dissimilar letters are significantly different ($p < 0.05$).

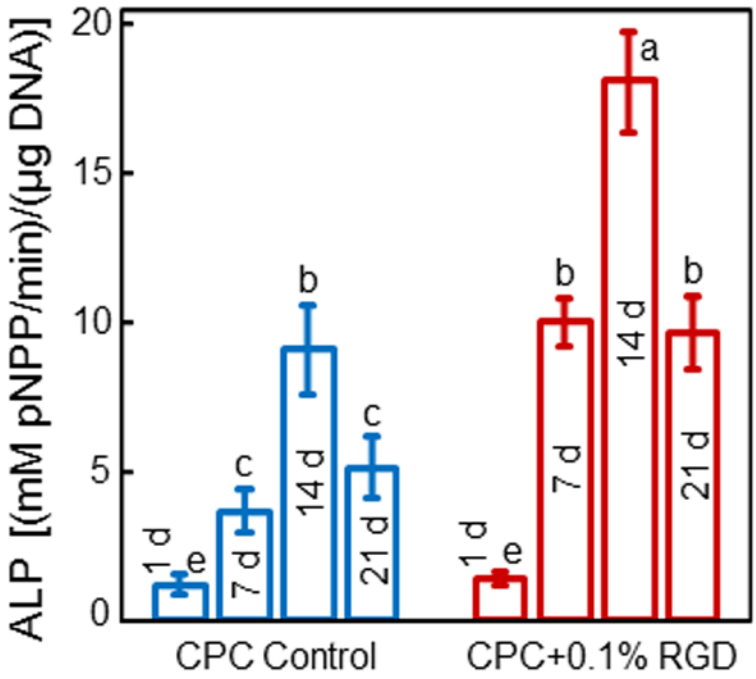

Fig. 5.

ALP activity of hUCMSCs inside macroporous CPC control and CPC + 0.1% RGD scaffolds (mean ± sd; n = 5). Values indicated by dissimilar letters are significantly different ($p < 0.05$). The ALP protein synthesis peaked at 14 d for both types of constructs. However, the ALP peak for CPC + 0.1% RGD was 2-fold that of CPC control ($p < 0.01$), indicating that RGD incorporation in CPC scaffold enhanced the osteogenic differentiation of hUCMSCs.

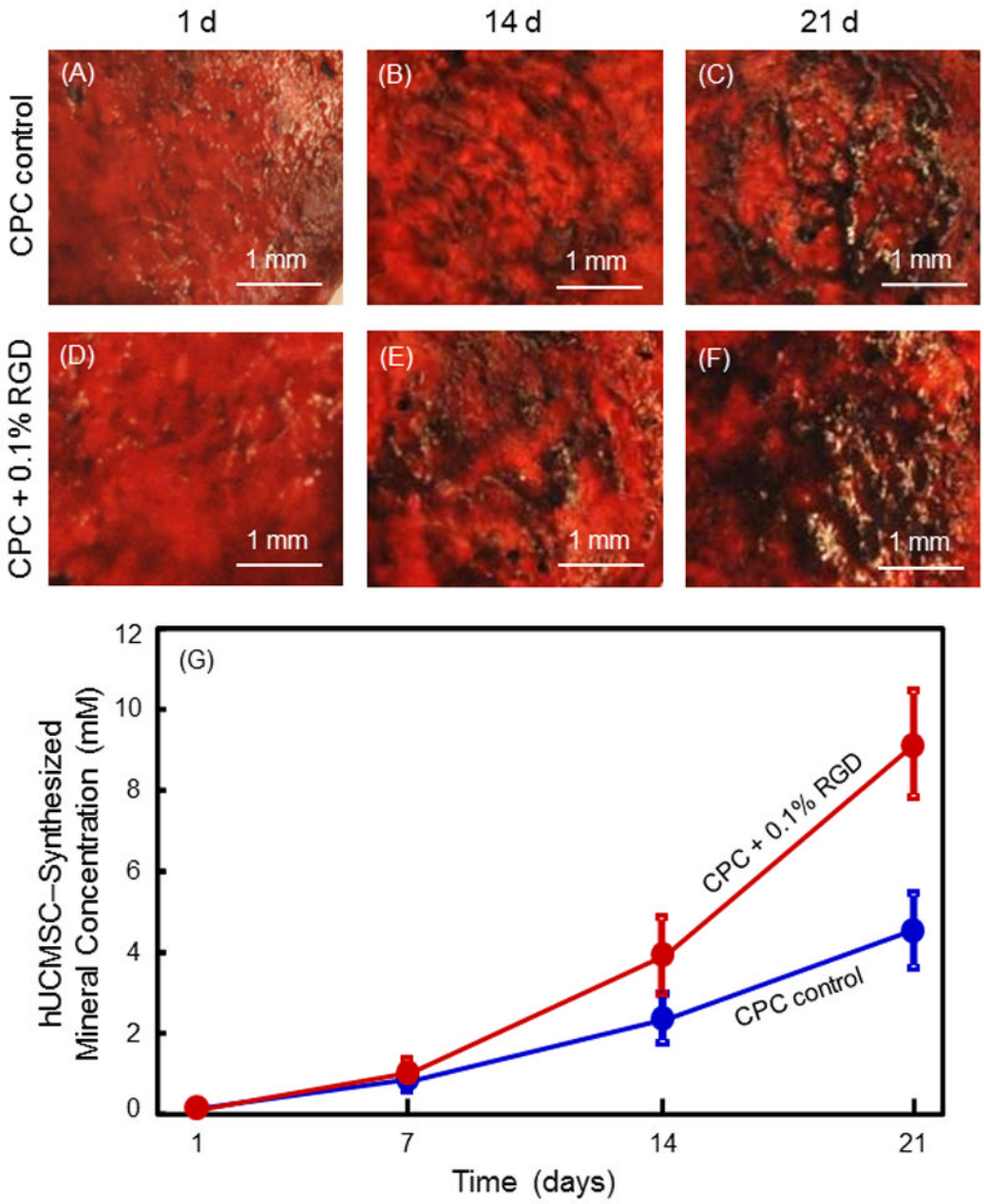

Fig. 6.

Mineral synthesis by hUCMSCs inside the constructs. (A–F) ARS staining of minerals synthesized by hUCMSCs inside CPC. The left label indicates the construct type. The top indicates culture time. CPC matrix was stained a red color. With the released hUCMSCs synthesizing a bone mineral matrix, the staining became a thicker and darker red. There was a layer of new mineral matrix synthesized by the cells covering the CPC, and this new matrix was thicker on CPC + 0.1% RGD than that on CPC control. The mineral data from the osteogenesis assay are plotted in (G) (mean ± sd; n = 5). Values with dissimilar letters are significantly different ($p < 0.05$).

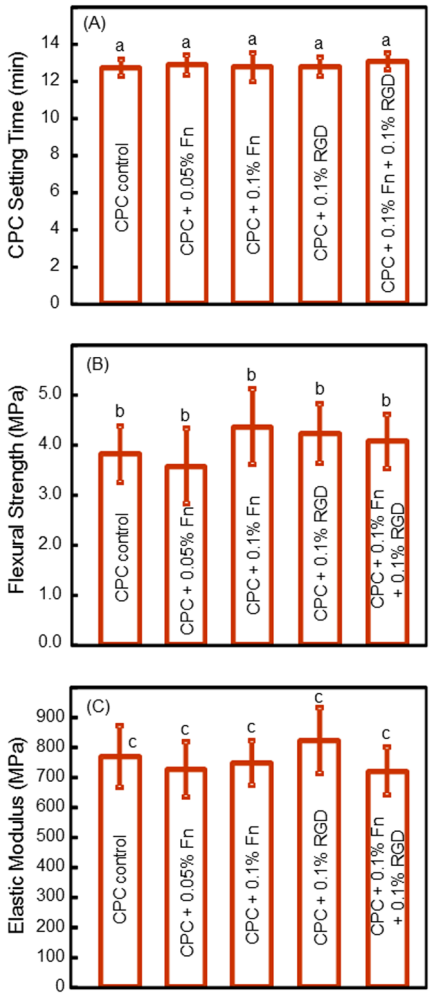

Fig. 7.

Setting time and mechanical properties of CPC (mean ± sd; n = 5). (A) CPC setting time, (B) flexural strength, and (C) elastic modulus. In each plot, values with the same letter are not significantly different ($p > 0.1$).